University of Baghdad
College of Engineering
JOURNAL OF ENGINEERING

Journal of Engineering
journal homepage: www.joe.uobaghdad.edu.iq
Number 3 Volume 27 March 2021

Civil and Architectural Engineering

Effect of Web Stiffeners on The Flexural Behavior of Composite GFRP-Concrete Beam Under Impact Load

Safaa I. Ali*
Ph.D. student
College of Engineering – University of Baghdad
Iraq, Baghdad
E-mail:safaa.ib90@gmail.com

Abbas A. Allawi
Prof Dr.
College of Engineering – University of Baghdad
Iraq, Baghdad
E-mail:a.allawi@uobaghdad.edu.iq

ABSTRACT

In this paper, numerical and experimental studies on the elastic behavior of glass fiber reinforced polymer (GFRP) with stiffeners in the GFRP section's web (to prevent local buckling) are presented. The GFRP profiles were connected to the concrete deck slab by shear connectors. Two full-scale simply supported composite beams (with and without stiffeners) were tested under impact load (three-point load) to assess its structural response. The results proved that the maximum impact force, maximum deflection, damping time, and damping ratio of the composite beam were affected by the GFRP stiffeners. The experimental results indicated that the damping ratio and deflection were diminished compared to hybrid beam without stiffeners by 16% and 22%, respectively, and increasing damping time by 26%. Finite element models were used to study pre-failure behavior. The numerical modeling results showed good agreement with experimental data in terms of loading path and final load. The damping ratio and midspan deflection values were greater than the experimental values by 6% and 12%, respectively.

Keywords: Glass fiber reinforced plastics (GFRP); Concrete; Shear connection; Hybrid beams; Composite beam; Pultruded FRP.

تأثير التقوية بأستخدام عناصر الـ GFRP على سلوك الانحناء للعتبات المركبة تحت تأثير الاحمال الصدمية

عباس عبد المجيد علاوي
استاذ دكتور
كلية الهندسة / جامعة بغداد

***صفاء ابرهيم علي**
طالب دكتوراه
كلية الهندسة / جامعة بغداد

الخلاصة

في هذا البحث ، تم عرض دراسات تجريبية ورقمية على السلوك المرن للبوليمر المقوى بالألياف الزجاجية (GFRP) مع تقوية قسم GFRP لمنع الانثناء المحلي. كان GFRP مرتبطًا بالبلاطة الخرسانية بواسطة

*Corresponding author
Peer review under the responsibility of University of Baghdad.
https://doi.org/10.31026/j.eng.2021.03.06

Article received: 22/9/2020
Article accepted: 25/10/2020
Article published:1/3/2021

موصلات القص. تم اختبار حزمتين كاملتين مسندة إسنادا بسيطا تحت أحمال الصدم ، وتم إجراء اختبار الانحناء من ثلاث نقاط لتقييم استجابته الهيكلية. أثبتت النتائج أن أقصى قوة صدمة، وأقصى هطول، ووقت ونسبة الإخماد للحزمة المركبة قد تأثرت بأجزاء التقوية بالـ GFRP. وأوضحت النتائج التجريبية أن نسبة الإخماد والهطول في منصف العتبة المركبة تقلص بنسبة 33٪ و 22٪ على التوالي. تم استخدام نماذج العناصر المحددة لدراسة سلوك ما قبل الفشل. أظهرت النتائج العددية توافق جيد مع البيانات التجريبية من حيث مسار التحميل والحمل النهائي. كانت نسبة الإخماد وقيم الهطول في منصف العتبة المركبة أكبر من القيم التجريبية بنسبة 6٪ و 12٪ على التوالي. تم تقييم طرق التصميم بناءً على المعيار الأمريكي، والذي أشار إلى دقتها المرضية.

الكلمات الرئيسية: البلاستيك المقوى بالألياف الزجاجية (GFRP) ؛ الخرسانة؛ موصلات القص، العتبات الهجينة.

Abbreviations	
FRP	Fiber Reinforced Polymer
GFRP	GFRP Glass Fiber Reinforced Polymer
CFRP	CFRP Carbon Fiber Reinforced Polymer
C-GFRP	Hybrid Carbon and Glass Fiber Reinforced Polymer
GF	Glass Fiber
CF	Carbon Fiber
LC	Lightweight Concrete

1. INTRODUCTION

Glass fiber reinforced polymer (GFRP), also known as enhanced composite material (ACM), is a composite made of a matrix fiber-reinforced polymer resin matrix (usually glass, carbon, basalt, or aramid) **(Abbas et al., 2017).** The polymer is usually an epoxy resin, vinyl or thermoplastic polyester, or phenol-formaldehyde resin. In recent years, improved durability and high construction speed of flooring systems have led to the exploration of new structural solutions, and FRP and GFRP increase in particular due to their durability, low weight, ease of installation, greater durability in harsh environments, and low maintenance requirements **(Keller, 2002; Seible et al., 1999).** But due to the low strength of the material, high initial costs, and lack of design codes, FRP materials are not widely used as load-bearing elements. However, the alternative use of pultruded GFRP profiles in combination with concrete in hybrid structural elements creates very interesting and immediate opportunities either for the rehabilitation of degraded structural elements or for new structures. The strength of the FRP fragment is mainly determined by the type of fiber and its orientation, amount, and location. There are many industrial FRP products used in civil/structural engineering applications.

2. LITERATURE REVIEW

Although the current repair and reinforcement of RC structures have great potential for the use of advanced composite materials, the development of new structural systems and the directional behavior, lightness, and high mechanical properties of GFRP materials are compared with conventional materials (especially concrete (cheaper and more The combination of the most relevant properties of heavy materials)) still

represents great potential. To this end, several different hybrid concepts have been proposed and successfully tested by different authors. Recently, another hybrid solution was used on the surface of two multi-field bridges in the United States **(Seible et al., 1999)**. This hybrid system consists of pultruded FRP roof panels with a corrugated profile and used in fixed locations. After the concrete is hardened, it can also be used as a tensile reinforcement **(Joao R Correia et al., 2007).** A hybrid sandwich solution for use on bridge decks has been proposed. The solution consists of GFRP sheet metal and T-beam (used to tighten the skin) (also used as a permanent mold), lightweight concrete (LC) core, and high Compression composition of performance reinforced concrete skin. A total of eight 3.0 m long hybrid beams were tested in a three-point bending test.

In half of the girders, only the mechanical connection of T-beams provides shear force. Also, at the interface between the GFRP board and the new lightweight concrete, a layer of epoxy glue is applied on the other half of the beam. Both types of beams failed due to shear in the LC core, but the relevant interface's final load was 104% higher than the average. In addition, a premature detachment was observed at the interface between the unbundled GFRP plate and the LC, which indicates the ultimate ductile failure. On the contrary, the bound air interface remains intact, but the failure is fragile and sudden. **(Swolfs et al., 2014)** reviewed the hybridization of compounds containing GF and CF. They included the basic mechanism of hybrid effects and mechanical properties' determination due to tensile, bending, impact, and fatigue loads to optimize hybrid composite materials' designs. **(Hai et al., 2010)** Bending tests were performed on C-GFRP I hybrid beams with different CF content on the flange. Although the bending stiffness increased steadily with the amount of CF, the maximum load-bearing capacity (33%) of the average CF content was obtained (i.e., to obtain a higher amount of CF reinforcement, the maximum load was reduced). GFRP hybrid beams can more accurately and completely evaluate the benefits of inserting CF into exposed GFRP profiles. In addition, this article usually does not introduce height models.

The special hybrid beams of CFRP and GFRP layers are given with simple and complex components **(Mutsuioshi et al., 2011).** Due to the mesh's flattening, only the profile cannot be bent, and the composite profile has better performance in all aspects. **(Gonilha et al., 2014)** found that the increased strength of the concrete floor slab in the GFRP-FSRSCc unit of the prototype floor caused the system to bend and prevent failure. **(M.M.Correia, 2012; Nunes et al., 2016)** proposed experimental and numerical studies on the structural characteristics of GFRP beams with unidirectional CF pads and C-GFRP hybrid beams. Due to the CF pad's delamination on the compression flange, the hybrid beam fails prematurely. In terms of stiffness and final load, a good agreement was observed between the experimental results and the numerical finite element model, but the progressive delamination and failure behavior of hybrid beams were not resolved. **(Nunes et al., 2016)** provided experimental, numerical, and analytical studies on the bending behavior of FRP and GF and CF fibers bonded together and integrated into the polyester matrix. GFRP and five series of C-GFRP hybrid profiles, with different types and structures of CF, reinforced materials, tested four-point bending to evaluate their structural response to failure. The experimental results confirmed the effectiveness of hybridization in improving bending stiffness. **(Gong et al., 2018)** reports on the results of a numerical investigation on the impact behavior of a hybrid GFRP-concrete beam subjected to low-velocity impacts

with different impact energy levels. A nonlinear finite element model has been developed using the commercial software ABAQUS/Explicit to simulate the hybrid beam's impact performance under impact loading. The numerical results, including the impact loading history, failure modes, and impact performance, are compared to the experimental results., Six hybrid beams, which consisted of rectangular hollow section pultruded GFRP profiles filled with high-performance concrete, were tested along the weak axis. The hybrid beams were subjected to a concentrated impact load by a cylindrical impactor for three ascending impact energy levels. The agreement between the numerical and experimental results indicates that the developed numerical model is capable of analyzing the impact behavior of such a hybrid GFRP-concrete system. **(Abbas and Safaa, 2020)** examined the effect of glass fiber reinforced polymer (GFRP) section and compressive strength of concrete in composite beams under static and impacted loads. Modeling was performed, and the obtained results were compared with the test results, and their compatibility was evaluated. Bending characteristics were affected by the strength of concrete under the impact loading case. It increased the maximum impact force and damping time at a ratio of 59% and reduced the damping ratio by 47% compared to the reference hybrid beam. There was an increase in all the parameters under static loading, including the maximum load, ductility, and stiffness. Mid-span deflection was reduced by 25% under static and impact loads. Finite element analysis was performed by using the ABAQUS software. The midspan deflection value was greater than the experimental values by 6% and 3% for impact and static loads, respectively, and all other results showed a high rate of agreement with the obtained test results.

3. EXPERIMENTAL PROGRAM

The experimental procedure aims to study the behavior of GFRP-concrete hybrid beams in simple supporting structural elements. Two-hybrid beams (one strengthens with stiffeners and another without stiffeners) with a total length of 3000 mm are subjected to an impact load at the center. The behavior of GFRP concrete mixed solutions in structural elements that only impact loads were a study. Each hybrid beam consisting of the concrete slab with a width of 500 mm and a thickness of 80 mm was supported by minimum reinforcement. The concrete slab was connected to the GFRP section by shear connectors (hook) and stiffened with GFRP stiffeners cutting from the GFRP section with a length of 130 mm, a width of 25 mm , and thickness of 10 mm. Details and dimensions of the hybrid beam are shown in **Fig 2**.

The designations of the specimens were as follows

CN=Composite beam without Stiffeners.

CS=Composite beam with Stiffeners.

Dimensions Concrete Deck:

Referring to Chapter I, Sec.I3.1a of "Specification for Structural Steel Buildings: ANSI/AISC360-10" (Manual, 2005) issued by the American Institute of Steel Construction (AISC), the dimensions of the concrete deck for use in hybrid beams research were selected. It states that "The effective width of the concrete slab shall be the sum of the effective widths for each side of the beam centerline, each of which shall not exceed:

(1) One-eighth of the beam span, center-to-center of supports;

(2) One-half the distance to the centerline of the adjacent beam; or
(3) The distance to the edge of the slab".
The first item is the only one applicable to the current study. So, with a beam length of 3000 mm (span = 2600 mm), the following value is calculated:
$b_{eff} = 2 \times \text{span} / 8 = 2 \times 2600/8 = 650\ \text{mm}$
An effective concrete deck width b_{eff} of 500 mm will be used.

4. MATERIALS AND METHODS

The pultruded GFRP I profile used in the bending test is made of a polyester matrix reinforced with polyester glass fiber (inorganic content is 61%, by weight) and has the following nominal dimensions: height ($h = 150$ mm), width ($b = 100$ mm) and thickness of the web and flanges ($t_w = t_f = 10$ mm). The tensile, compressive, bending, and shear properties were determined using an extensive mechanical characteristic based on experiments with coupons cut from the original profile. The longitudinal bend coefficient ($E_p = 33$ GPa) and shear modulus ($G_p = 3.3$ GPa) were determined during a comprehensive test carried out on a profile similar to that used in the tested beams (Correia, 2004). The average compressive strength ($f_c' = 25\ MPa$) and Young's modulus ($E_c = 24\ GPa$) of concrete were experimentally determined. The shear connection was provided by an inverted U-shaped bolt (hook).

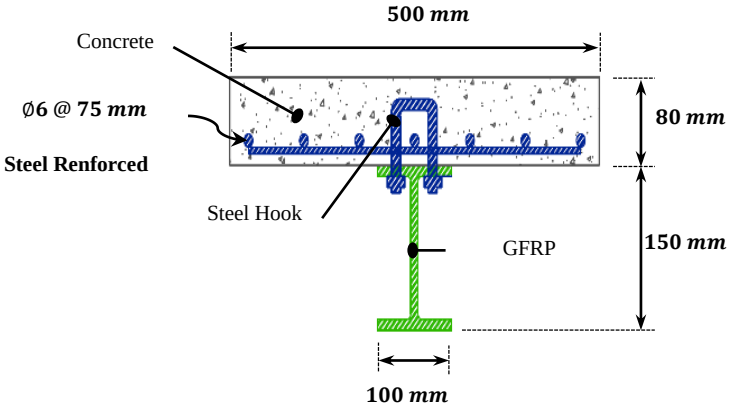

Figure 1.GFRP–concrete hybrid section geometry (dimensions in mm).

4.1 GFRP Pultruded I-Section

The experimental procedure's I profile consists of a pulsed polyester matrix reinforced with E glass fibers. Coupons cut from the original profile were used for extensive mechanical characterization regarding tensile, compressive, flexural, and shear properties **(Correia, 2004) (Branco et al., 2003).** THE I-shaped GFRP section is shown in **Fig 1**.

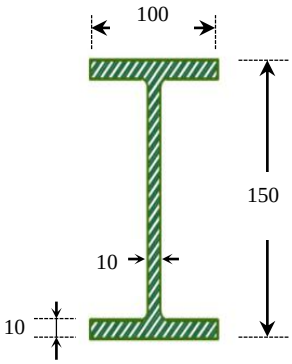

Figure 2. cross section details (all dimensions in millimeter).

4.2 GFRP Stiffeners

Stiffeners are secondary plates or sections attached to beam webs or flanges to stiffen them against out-of-plane deformations. Since the ultimate bending stress of the GFRP section adjusts the local buckling of its extraordinary flange, GFRP stiffeners are provided to prevent buckling when subjected to load during the test. They were fixed onto the web between flanges using the epoxy resin adhesive that was spread on three stiffener pieces using a steel blade and glued to the section. **Fig. 3** shows the stiffener and process to fix it in position, The specification of the epoxy types is listed in **Table 1** as supplied by the manufacture.

Table 1. Epoxy Resin Adhesive Technical Data.

Compressive Strength (MPa)	Tensile Strength (MPa)	Flexural Strength (MPa)	Modulus of Elasticity (MPa)	Bond Strength (MPa)	Elongation, (%)	Final Curing
70	30	20 - 26	4500	> 4	0.9	7 days

4.3 Shear Connectors

U-shaped inverted (hook), 12 mm diameter with ultimate tensile stress (**Fig. 4**) (800 MPa) were used to achieve the connection between the GFRP and the concrete deck slab. The adhesion between GFRP and concrete was negligible. Therefore, the entire transverse connection was provided by mechanical contact. A punching shear test was conducted to analyze the relationship between GFRP and concrete and was used to calculate the distance between the shear connectors. In punching tests, the flanges of the sections of the GFRP used in the hybrid beam were hooked to double-prisms concrete. (**Fig. 5** and **6**). Then the profile was loaded as compressed to failure. The load was applied monotonously until the separation of the substance occurred, with the results given to joint stiffness evaluated according to the definition presented **(Johnson and May 1975).** The separation of the material occurred suddenly due to the hooks' destruction, with a maximum load of only 159 kN (79.5 kN / mm per flange). During testing at high loads, the deformation increased significantly. The high-pressure stress at the edge in front of the hooks indicates that fracture is inevitable.

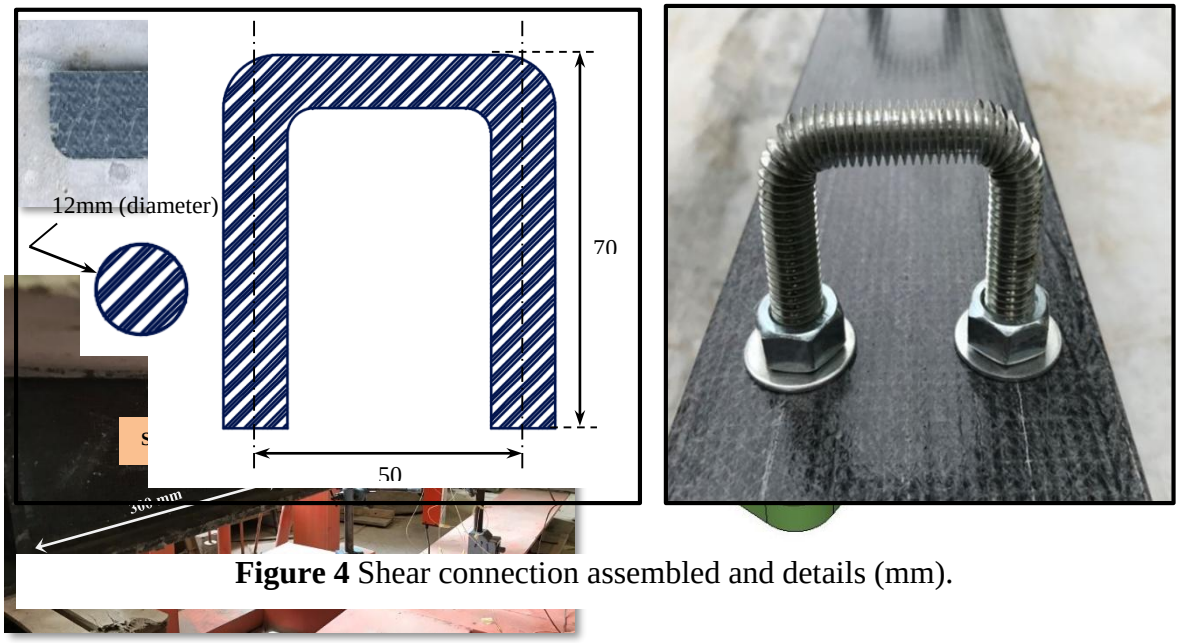

Figure 4 Shear connection assembled and details (mm).

Figure 3. Details of the stiffener and the process of fixing it in position.

5. PROPERTIES OF THE HYBRID BEAMS

The cross-section of the hybrid beam is related to the priority application of this type of structural element, which is, in the restoration of degraded structures, it is selected as a simple support element and developed according to the previously developed positive

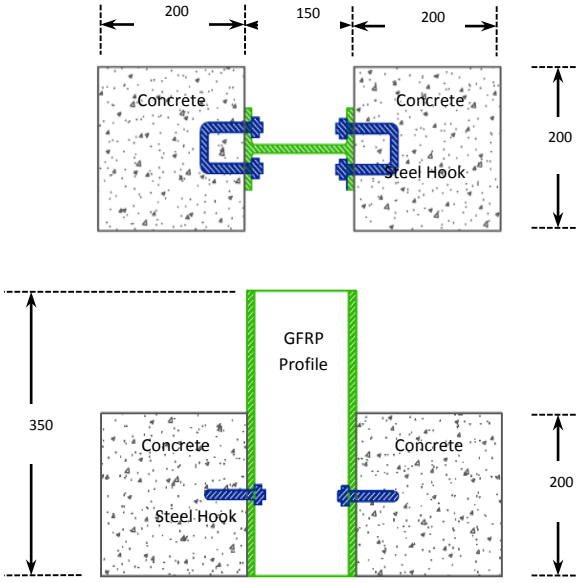

Figure 5. Geometry of the test specimen (mm): plan (top) and section (bottom).

Figure 6. Shear connection test setup.

bending equation **(Joao R Correia et al., 2007)**. Therefore, in this structural system, it is necessary to realize the compression fracture of concrete with a neutral axis in the concrete slab, and at the same time make full use of the material properties of the GFRP profile, which will cause bending fracture at the local torsion of the lower profile flange. The horizontal plastic rod steel is placed on top of the concrete. Assuming that the critical local torsional curvature (shown in **(Correia, 2004)**) was previously performed, which was supported simply by the span GFRP profile (from the same batch of configurations used to manufacture hybrid beams), (laterally adjusted along its length)

6. EXPERIMENTAL SETUP AND TEST PROCEDURE

The test setup is illustrated in **Fig. 7**. A 3000 mm long FRP beam was tested in a simple supported 2600 mm span configuration. In the case of three-point bending, the beam is tested to withstand a single load (impact load) in the span's center. The end beam is compacted with two sets of rollers, and a 25 kg steel block is used to apply a load, and the load falls freely on the sample just in the middle of the test frame without any external force.

The instrument used to measure the average range deviation of each time step and placed at the bottom of each sample is a laser sensor. In contrast, a linear variable displacement sensor (LVDT) is used to measure the mid-range edge deviation. Two types of load cells were used, a load cell with the capacity of 100 kN was used to record the applied load that was developed by dropping a mass and a Philips load cell (PR 6200/14/A) with the capacity of 100 kN placed under one support to measure the load under support, as shown in **Fig. 8**.

Figure 7 steel frames for impact test.

Figure 8 load cells.

RESULTS AND DISCUSSION

6.1 Experimental Results

To study the effect of impact loads on composite beams' strength and performance (profiled GFRP I-Section and concrete deck slabs), two simply supported composite beams were tested under impact loading (low-velocity impact). Strong steel frame and heavy to hold rigidly during impact loading by connected all structural elements to build the frame as shown in **Fig 9** show sketch for the steel frame that manufactured to

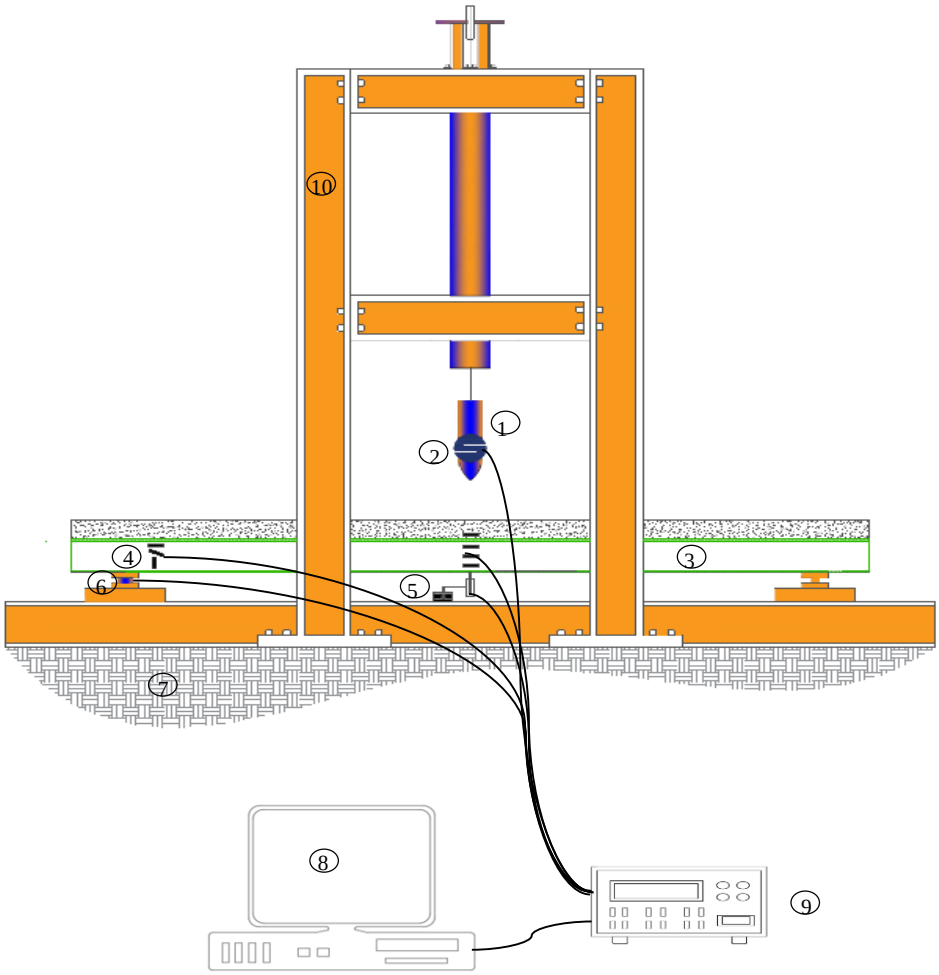

1- **Impact mass.**
2- **Load cell.**
3- **Test Beam.**
4- **Strain Gauges.**
5- **LVDT.**
6- **Load cell under support.**
7- **Rigid floor.**
8- **Computer.**
9- **Data logger.**
10- **Frame**

Figure 9 .Impact test Machine.

use for impact tests. Were designed to allow observing the specimens from the bottom surface to show developing failure during testing. Steel mass of 25 kg is provided and dropped freely without any external force to the specimen that was placed accurately in the middle of the testing frame.

According to the tests' results with the accepted parameters, the observed and recorded points of the tests were as follows.
The short duration of applied loads was the main difference between impact and static tests. The sample was initially placed on the steel frame testing machine, and then deflection sensors, force sensors, and LVDT were set at certain points.
In general, the applied force, deflection, and tension behavior were not mathematically linear, and there were many different points of view so that the results (readings) changed in value over time. Initially, the readings were of little value because they were used for a short time. At a certain time, which depends on different variables, the readings changed in value, and many of these readings took place at times and then disappeared. Test results showed that the peak impact force and mid-span deflection increased as the height of freely dropped mass increased the stroked velocity.
Cracks occurring on the concrete surface due to the impact test were local cracks in and around the drop zone. These cracks were not considered residual for static tests. The cracks for all the samples were the same in configuration but differed in intensity. As the spacing between shear connections decreased, cracking reduced as well.

6.1.1 Maximum impact force and maximum deflection

Table 2 lists the results of the beams tested, maximum impact force, maximum deflection as a function of time, penetration to the upper face of the beam and residual deformation. Bending time history and deformation have different values, depending on the evolution of the spacing between stiffeners, reduced the maximum deformation of the samples compared to the reference by 22%, and the impact force increased due to the capacity of the composite beams to absorb a larger amount of energy before failure occurs.

Table 2. Specimen's test results.

Drop height (mm)	Name of specimen	Maximum Impact force (kN)	Maximum deflection (mm)	Penetration depth (mm)	Residual deflection (mm)
100	CN	9.95	5.73	-	0.72
	CS	9.6	4	-	0.8
500	CN	19.1	10.45	0.2	4.1
	CS	23	9	0.3	4.9
1000	CN	25.7	14.74	0.9	7.1
	CS	34	12.3	1	7
1500	CN	32.43	21.77	2.2	11.44
	CS	49.4	15.4	1.9	11.1
2000	CN	46.5	20.65	4	14.9
	CS	50.1	19.68	4	13.3

6.1.2 Load under support

The impact load is measured by stabilizing the load cell sensor under support. Using stiffeners in the composite beams reduced the absorption by 40% due to the composite beams' increased stiffness (**Fig. 10**).

6.1.3 Damping time and damping ratio

These results were obtained by using the LVDT sensor by installing it below the middle of the beam. The time needed to reach 10% of the maximum deflection is called damping time, that is, the time required to reach 90% of damping **(Clough and Penzien, 1995)**. The damping ratio is known as the ratio of the viscous damping coefficient to the critical damping coefficient. It is designated by ζ (zeta), and it was particularly important in the **(Alciatore, 2007)** study **(Allawi and Al Mukhtar, 2016).**

Table 3. Damping time, and percentage of increase in it compared with reference hybrid beam.

Specimen designation	Damping Time (Sec.)	Increasing in Damping Time (%)
CN	1.5	-
CS	1.9	26.67

Table 4. Damping Ratio, and percentage of decreasing in it compared with reference hybrid beam.

Specimen designation	Damping ratio (%)	Decreasing in Damping ratio (%)
CN	0.5	-
CS	0.42	16.0

- The experimental measure of damping ratio - logarithmic decrement

In this relationship, deflection is reduced from one peak to another until reset. A suitable way to measure the damping present in the system is to measure free oscillations' decay rate **(Tveten et al., 2014).** The larger damping, the greater is the rate of decay, and it is calculated using the following equations:

$$\delta = \frac{1}{n-m} ln\left(\frac{v_m}{v_n}\right) \quad (1)$$

$$\zeta = \sqrt{\frac{\delta^2}{4\pi^2+\delta^2}} \quad (2)$$

where $(n)$and (m) represent deflection at peak (υ_m, υ_n), respectively,(**Fig. 12**).
The stiffeners' presence increases the damping time of the hybrid beam compared to the hybrid beam without stiffeners (CS) by ratio (26.67%), which are, as shown in **Table 3**.
The stiffeners resulted in a 16% reduction in the damping ratio, which causes an inverse relationship between the damping time and the damping ratio (**Fig. 11**) and (**Table 4**).

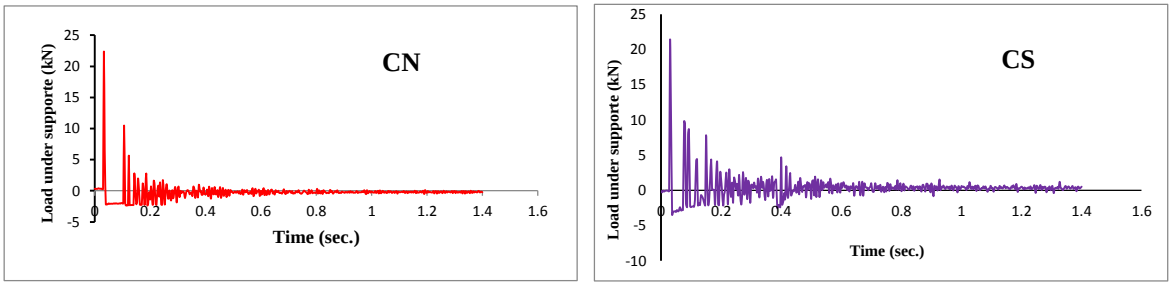

Figure 10 .Relationship of load under support for hybrid beams.

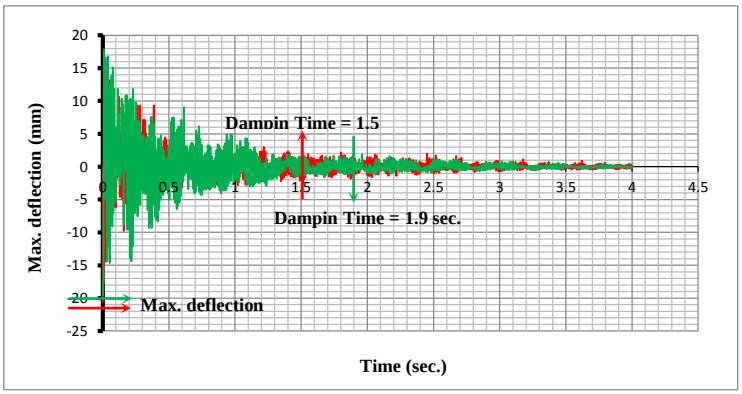

Figure 11 The relationship between deflection and the time for the hybrid beam (CN) compared to the reference hybrid beam (CS) and the damping time.

.

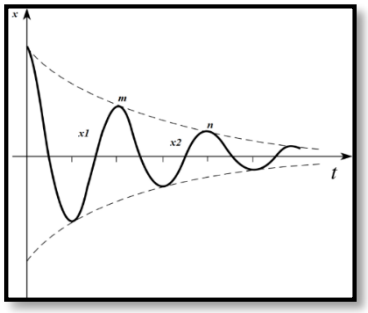

Figure 12. Rate of oscillation decay.

7. NUMERICAL MODELING

7.1 Finite Element Method

A numerical approach was adopted for finite elements: three-dimensional modeling composite beams (GFRP) were tested under impact and static loads. The ultimate analysis of elements with the ABAQUS version 6.14 package consisted of real-time experimental simulation on beams to be examined.

The composite beams, consisting of GFRP, deck slab, and shear connectors, were modeled under 3D stress elements for all the components, except for reinforcement steel, which was modeled using standard 2D elements.

The concrete volume is represented by a solid brick element with eight nodes (C3D8R) and integration points 2x2x2. The longitudinal and transverse reinforcement of these beams is modeled using built-in reinforcement of linear 3D truss elements with 2 nodes (T3D2). The solid element with eight nodes is also used to model the steel plate under the applied load and resistance response (**Fig. 13**). In this numerical analysis, it is

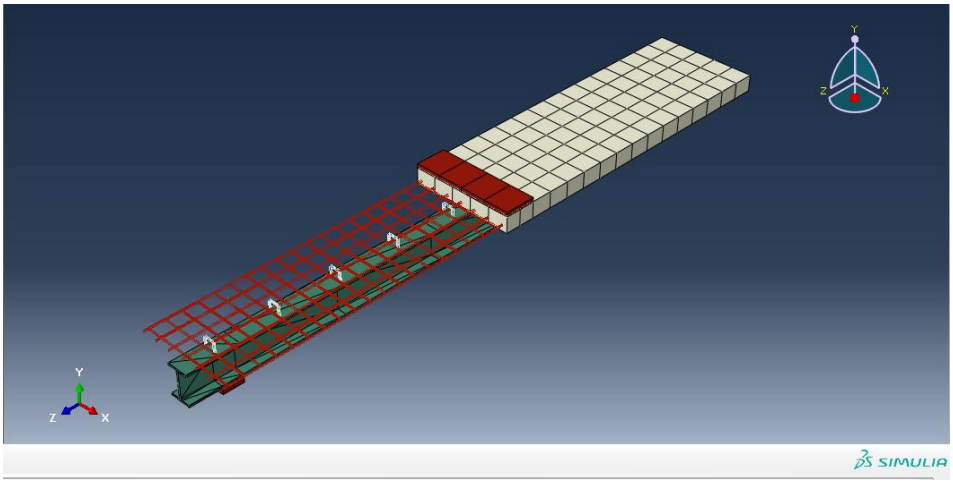

Figure 13. Model meshing for the composite beam.

worth noting that a perfect connection (i.e., complete compatibility) between the surrounding concrete and steel is assumed. Use the damaged plasticity model (DPM) for analysis. This model combines unbound multi-solid plasticity and scalar (isotropic) elasticity to describe the irreversible failure that occurs during the fracture process. This model's two main failure mechanisms are the cracking in the tensile and compression fracture of concrete.

Numerical methods are the most effective engineering analysis techniques that can handle complex geometric shapes. Among many methods, finite element analysis (FEA) is one of the most versatile and comprehensive techniques currently available to engineers **(Srinivas et al., 2010)** and **(Abbas. and Shakir, 2015).**

7.2 Impact Loading

ABAQUS uses the experimental study's load-time curves to check parameters such as deflection, strain, and stresses as a function of time for analysis. A hollow solution was used to solve the equation set to identify the unknown variable (this method was included in the ABAQUS program). Multiple models ABAQUS adopts a finite element

approach to simulate some of the tested beams in order to verify the complete operation of the hybrid beams subjected to static and impact loads. The maximum transient intermediate defect is an important indicator for assessing the damage levels caused by hybrid beams exposed to shocks. The results of the numerical models are related to the test results. Therefore, the supported load is more appropriate than the maximum effect and the specific result of maximum deflation (**Fig. 14**).

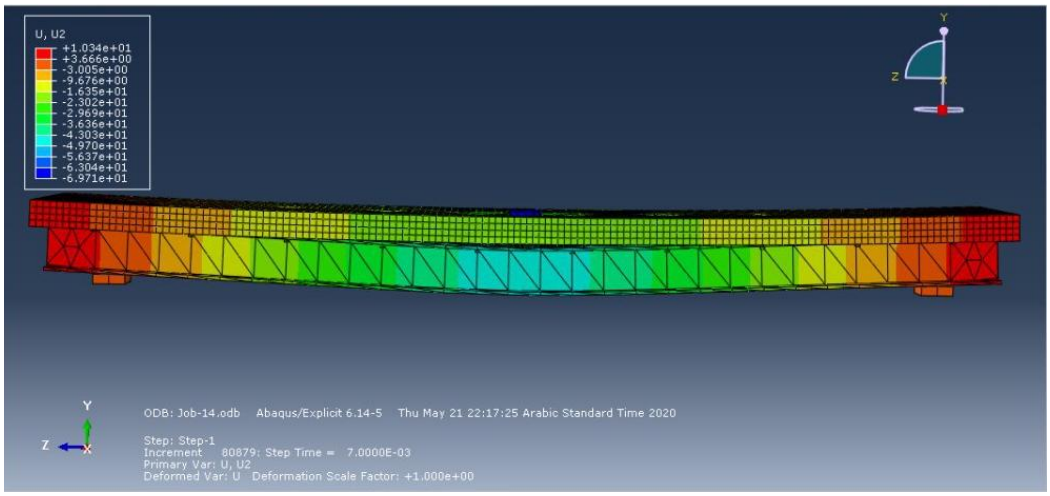

Figure 14. Analysis results of mid-span deflection of the hybrid beam under impact load.

According to FEA results, CN beam maximum mid-span deflection was 19.1 mm (as shown in **Table 5** compared to 20.65 mm of the experimental test. Load under support was 24.2 kN, while it was 22.4 kN in experimental results for the hybrid beam (CN). **Fig 15** shows a comparison of load under support, which indicates a good agreement between the experimental results and those of FEA.

Table 5 summary of all hybrid beams analysis result with comparison (impact force, maximum deflection, and load under support).

Beam Designation	Experimental			FEA (ABAQUS)			Maximum Impact force (%) EXP/FEA.	Maximum deflection (%) EXP/FEA	Load under support (%) EXP/FEA
	Maximum Impact force (kN)	Maximum deflection (mm)	Load under support (kN)	Maximum Impact force (kN)	Maximum deflection (mm)	Load under support (kN)			
CN	46.5	20.65	22.4	44.7	19.1	24.2	1.04	1.08	1.00
CS	50.1	19.68	21.1	49.1	18.5	24.55	1.02	1.06	0.86

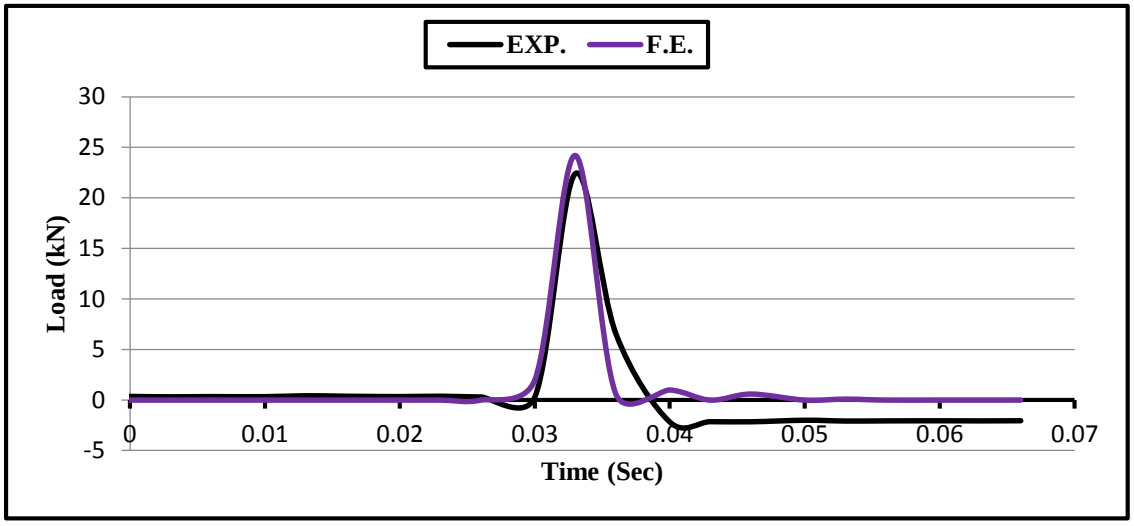

Figure 15. Experimental versus finite element load under support curves of the hybrid beam (CN).

8. CONCLUSIONS

The design of pultruded GFRP beams is usually affected by deformation or instability. In order to make better use of material properties, GFRP profiles can be used in combination with concrete elements and have multiple advantages related to the stiffness and strength of the structural elements, which results in the solution being particularly suitable for degraded floor restoration and new construction projects. This article introduces a structural solution analysis and experimental study combining PFRP pultruded profiles with concrete elements in GFRP-concrete mixed structural elements. The following are the main conclusions:

1. GFRP–concrete hybrid beams with reasonable stiffness, high strength, and low self-weight are a viable structural solution that can be used in repair strengthening or even in new construction projects.
2. The ultimate strength and deflections of the GFRP hybrid beams can be predicted with good precision using the proposed analysis methods where shear deformation and interconnecting slip must be considered.
3. The stiffeners of GFRP–concrete hybrid beams increased the strength of composite beams and damping time and reduced the damping ratio.
4. The using stiffeners were considered useful methods to enhance the composite beams impact forceand Damping time by (22 and 26.67) % respectively, and decreasing deflection at mid-span and Damping ratio by (10 and 16%).
5. The similarity in modes of failure of the hybrid beams by interlaminar shear failure reflects a weakness in the region of the flange to the web junction of the GFRP section. This necessitates some measurements to be taken by manufacturers during the fabrication process to strengthen this region, whether related to fiber reinforcement or matrix resin content or using stiffeners in the GFRP section, which showed good performance when used.

REFERENCES

- Abbas, A., Safaa, I., 2020. Effect of concrete grade on the flexural behavior of composite GFRP Pultruded I-section beams under static and impact loading. Civil Engineering Journal.
- Abbas, R., ALSaleh, S., and Agil, A., 2017. Study the effect of microbial factor on the qualities and characteristics of Novolak composite material, reinforced glass fibers / Asbestos fibers., Journal of Engineering, 23(5), pp. 1-14. Available at: http://joe.uobaghdad.edu.iq/index.php/main/article/view/47 (Accessed: 6 October 2020).
- Abbas, R., and Shakir, H., 2015. Finite Element Investigation on Shear Lag in Composite Concrete-Steel Beams with Web Openings, Journal of Engineering, 21(3), pp. 11-33. Available at: http://joe.uobaghdad.edu.iq/index.php/main/article/view/453 (Accessed: 6 October 2020).
- Alciatore, D. G., 2007. Introduction to mechatronics and measurement systems. Tata McGraw-Hill Education.
- Allawi, A., and Al Mukhtar, A., 2016. The Use of the Artificial Damped Outrigger Systems in Tall RC Buildings Under Seismic Loading, Journal of Engineering, 22(4), pp. 30-49. Available at: http://joe.uobaghdad.edu.iq/index.php/main/article/view/231 (Accessed: 6 October 2020).
- Branco, F. A., Ferreira, J., and Correia, J. R., 2003. The use of GRC and GFRP-concrete beams in bridge decks. FRP Composites in Bridge Design and Civil Engineering, COBRAE Conference Proceedings, Porto.
- Clough, R. W., and Penzien, J., 1995. Dynamics of Structures, Computers & Structures. New York.
- Correia, J R., 2004. Glass fiber reinforced polymer (GFRP) pultruded profiles. Structural behaviour of GFRP-concrete hybrid beams. MSc Thesis, Instituto Superior Técnico, 2004 [in Portuguese].
- Correia, Joao R, Branco, F. A., and Ferreira, J. G., 2007. Flexural behaviour of GFRP–concrete hybrid beams with interconnection slip. Composite Structures, 77(1), 66–78.
- Correia, M. M., 2012. Structural behavior of pultruded GFRP profiles experimental study and numerical modeling. Technical University of Lisbon, Av. Rovisco Pais, 1001–1049.
- Gong, J., Zou, X., Shi, H., Jiang, C., and Li, Z., 2018. Numerical investigation of the nonlinear composite action of FRP-concrete hybrid beams/decks. Applied Sciences, 8(11), 2031.
- Gonilha, J. A., Correia, J. R., and Branco, F. A., 2014. Structural behaviour of a GFRP-concrete hybrid footbridge prototype: experimental tests and numerical and analytical simulations. Engineering Structures, 60, 11–22.
- Hai, N. D., Mutsuyoshi, H., Asamoto, S., and Matsui, T., 2010. Structural behavior of hybrid FRP composite I-beam. Construction and Building Materials, 24(6), 956–969.
- Johnson R. P. and. May I. M. (1975), Partial-interaction design of composite beams, Struct. Eng., vol. 8, no. 53.
- Keller, T., 2002. Fiber reinforced polymer materials in bridge construction. IABSE Symposium Report, 86(7), 119–126.
- Manual, S. C., 2005. American Institute of steel construction. Inc., Thirteenth Edition, First Print

- Mutsuyoshi, H., Hai, N. D., Shiroki, K., Aravinthan, T., and Manalo, A., 2011. Experimental investigation of HFRP composite beams. Proceedings of the 10th International Symposium of the Fiber Reinforced Polymer Reinforcement for Reinforced Concrete Structures (FRPRCS-10), 1(275), 219–243.
- Nunes, F., Correia, J. R., and Silvestre, N., 2016. Structural behavior of hybrid FRP pultruded beams: Experimental, numerical and analytical studies. Thin-Walled Structures, 106, 201–217.
- Seible, F., Karbhari, V. M., and Burgueño, R., 1999. Kings stormwater channel and I-5/Gilman bridges, USA. Structural Engineering International, 9(4), 250–253.
- Srinivas, P., KUMAR, S. K. C. D. R., and Paleti, S., 2010. Finite element analysis using ANSYS 11.0. PHI Learning Pvt. Ltd.
- Swolfs, Y., Gorbatikh, L., and Verpoest, I., 2014. Fiber hybridisation in polymer composites: A review Part A Applied science and manufacturing.
- Tweten, D. J., Ballard, Z., and Mann, B. P., 2014. Minimizing error in the logarithmic decrement method through uncertainty propagation. Journal of Sound and Vibration, 333(13), 2804–2811. https://DOI.org/10.1016/j.jsv.2014.02.024.